ELSEVIER

Journal of Photochemistry and Photobiology A: Chemistry 123 (1999) 25–30

Journal of
Photochemistry
and
Photobiology
A:Chemistry

Dewar pyridine studied by matrix isolation infrared spectroscopy and DFT calculation

Satoshi Kudoh, Masao Takayanagi, Munetaka Nakata*

Graduate School of BASE (Bio-Applications and Systems Engineering), Tokyo University of Agriculture and Technology, 3-5-8 Saiwai-cho, Fuchu, Tokyo 183-8509, Japan

Received 29 October 1998; received in revised form 5 January 1999; accepted 3 February 1999

Abstract

Infrared spectra of Dewar pyridine, produced from pyridine in an argon matrix by UV irradiation, have been measured by matrix-isolation infrared spectroscopy. Vibrational assignments have been performed with an aid of the DFT calculation, where the 6-31++G** basis set was used to optimize the geometrical structures. It has also been found that cyclobutadiene and HCN are produced by further photolysis of Dewar pyridine as well as by direct photodissociation of pyridine. The relative rate constants are estimated from the infrared intensity changes upon UV irradiation. © 1999 Elsevier Science S.A. All rights reserved.

Keywords: Dewar pyridine; Matrix isolation; Infrared spectra; Cyclobutadiene; Reaction mechanism

1. Introduction

Dewar benzene has been extensively studied in the fields of organic and physical chemistry since Dewar proposed it in 1866 [1]. This compound was first synthesized by Ward and Winshnok in 1968 [2]. The geometrical structure was determined by vibrational spectroscopy [3,4], gas electron diffraction [5], and microwave spectroscopy [6] in the 1970s. On the other hand, only a few studies of Dewar pyridine have been published until now. In 1973, Chapman et al. [7] proposed a possibility of existence of Dewar pyridine as an intermediate in the photolysis of pyridine, but no spectrum was shown. Recently, Johnstone and Sodeau [8] observed some new bands in infrared spectra of pyridine photolyzed at 253.7 nm in an argon matrix. They pointed out that it was possible to assign them to Dewar pyridine but could not arrive at any definitive conclusion.

Recently, the density functional theory, DFT, has been developed in various fields of chemistry. This method has resulted in a number of molecular structures of unstable species such as van der Waals clusters [9] and photoreaction intermediates [10] as well as conformational isomers [11–13] by a comparison of the calculated spectral patterns with the corresponding observed vibrational spectra. In the present study, we have applied the low-temperature matrix-isolation technique and the DFT method to study the geometrical structure for Dewar pyridine. Unlike Dewar benzene, two tautomers can be considered for Dewar pyridine, as shown in Fig. 1. Type I has a C–C bridging bond, and has no symmetry element, whereas Type II has a C–N bridging bond and has a symmetry plane. It should be possible to determine which tautomer is produced from pyridine by UV irradiation.

We also report infrared bands of cyclobutadiene and HCN upon long-time UV irradiation. From an analysis of the intensity changes of the infrared bands for Dewar pyridine and cyclobutadiene, we propose a reaction mechanism that cyclobutadiene and HCN are produced by secondary photolysis of Dewar pyridine as well as by direct photodissociation of pyridine. The relative rate constants estimated by a least-squares fitting are compared with each other and discussed.

2. Experimental

A sample of pyridine (C_5H_5N) (>99.9% purity), purchased from Wako Pure Chemicals, was used without further purification. A pyridine-d$_5$ sample (C_5D_5N) was purchased from Aldrich (99 atom%). The sample vapor was premixed with argon gas (Nippon Sanso, 99.9999% purity) in a glass bulb. The mixing ratio of pyridine/argon was ca. 1/2000. The premixed gas was deposited on a CsI

---

*Corresponding author. Tel.: +81-42-367-5618; fax: +81-42-367-5618; e-mail: necom@cc.tuat.ac.jp

PII: S1010-6030(99)00035-0

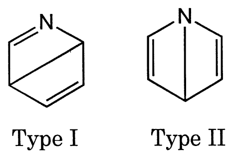

Fig. 1. Two possible tautomers of Dewar pyridine.

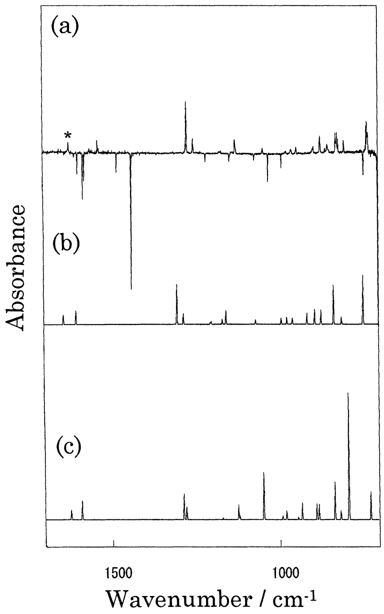

Fig. 2. Observed and calculated infrared spectra for C_5H_5N: (a) A difference spectrum between those observed before, and after, 10-min UV irradiation. Decreasing and increasing bands are due to pyridine and Dewar pyridine, respectively. A band at 1624 cm^{-1} marked with an asterisk is probably due to water impurity. (b) A spectral pattern of Type I for Dewar pyridine estimated by the DFT calculation. (c) A spectral pattern of Type II for Dewar pyridine estimated by the DFT calculation.

plate at 15 K cooled by a closed-cycle helium refrigeration unit. A superhigh-pressure mercury lamp was used to produce Dewar pyridine. The UV light was introduced on the matrix sample through a water filter of 50-mm diameter and 100-mm length and a quartz lens of 50 mm diameter and 200 mm focus length. Infrared spectra were measured with an FTIR spectrophotometer (JEOL, Model JIR-7000). The spectral resolution was 0.5 cm^{-1}, and the number of accumulations was 64. Other experimental details are reported elsewhere [9].

3. Results and discussion

3.1. Infrared spectrum of Dewar pyridine

An infrared spectrum of pyridine in an argon matrix was recorded after sample deposition before UV irradiation. Infrared bands of pyridine appearing at 1599, 1583, 1579, 1483, 1441, 1219, 1148, 1073, 1032, 991, 744, and 701 cm^{-1} agreed with the reported values [8] within a

Table 1
A comparison of vibrational wavenumbers (in cm^{-1}) and relative intensities for Dewar pyridine

C_5H_5N			C_5D_5N		
observed	calculated frequency	intensity	observed	calculated frequency	intensity
1562(w)[a]	1642	8		1612	11
1539(m),1535(w)	1605	11		1539	12
1278(w[d]),1275(s[b])	1306	33	1146(m[c])	1170	9
1255(m[d])	1287	9	1115(m[c])	1139	11
1178(w[d])	1207	1	1069(w[d])	1090	6
1172(w[d])	1204	2	992(m[c])	1015	11
1135(w[d])	1171	4	963(w[d])	983	3
1131(m[c])	1160	11	932(w[d])	948	1
1047(w[d])	1071	4	919(w[d])	936	3
977(w[d])	994	5	886(w[d])	904	4
962(w[d])	977	6	820(w[d])	836	3
	962	1		801	<1
946(w[d])	960	5	764(w[d])	773	5
897(w[d])	916	9	744(w[d])	759	2
874(m[c])	893	12	734(w[d])	753	3
859,852(w[d])	874	12			
828,823,819(m[c])	836	32			
802(m[c])	812	6			
735,733,729(s[b])	747	41			

[a] Relative intensities are in parentheses.
[b] Strong.
[c] Medium.
[d] Weak.

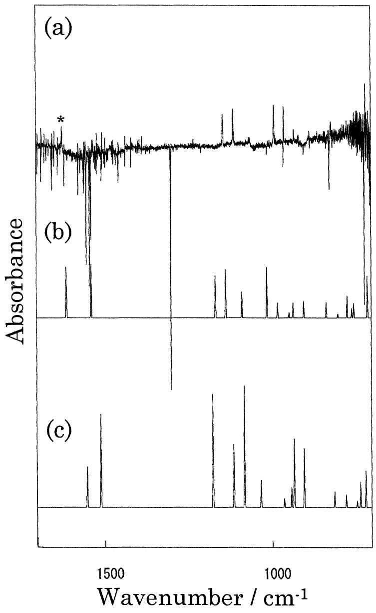

Fig. 3. Observed and calculated infrared spectra for C_5D_5N: See the legends of Fig. 2.

few wavenumbers. After measurement of the spectrum, the matrix sample was irradiated by UV light from a superhigh-pressure mercury lamp for 10 min. A difference spectrum between those measured before, and after, the irradiation is shown in Fig. 2(a), where decreasing and increasing bands were assigned to pyridine and a photoproduct, respectively. The wavenumbers of the photoproduct are summarized in Table 1 with their relative intensities.

A similar experiment was performed for completely deuterated pyridine-d_5. The infrared bands of C_5D_5N in an argon matrix were observed at 1553, 1544, 1539, 1302, 1211, 1014, 964, 903, 884, 835, 826, and 823 cm^{-1}. The difference spectrum is shown in Fig. 3(a). The signal-to-noise ratio was approximately twice as large as that for the normal species. The wavenumbers of the photoproduct are summarized in Table 1.

3.2. DFT calculation of Dewar pyridine

In order to determine the structures of the photoproducts, DFT calculations were performed using the GAUSSIAN 94 program [14] with the 6-31++G** basis set, where the hybrid density functional [15] was used in combination with the Lee, Yang, and Parr correlation functional (B3LYP) [16] to optimize the geometrical structures. The obtained geometrical structures for types I and II of Dewar pyridine are illustrated in Fig. 4.

Our calculations have shown the result that Type I is more stable by 9.1 kcal mol^{-1} than Type II. This is consistent with the results of ab initio calculations at the RHF/6-31G* level by Liu et al. [17] and at the MP2/DZP//HF/3-21G level by Jones et al. [18], where the energy difference between the tautomers was reported to be 13.6 kcal mol^{-1} in the former and 9.7 kcal mol^{-1} in the latter. Our results support the interpretation of Liu et al., who pointed out that Type II is more strained than Type I since the length of the C–N bridging bond for Type II is shorter than that of the C–C bridging bond for Type I. The bond lengths and bonded angles obtained in our calculation are similar to those reported in the former but are slightly different from those reported in the latter. For example, the results show the length of the C–C bridging bond for Type I is estimated to be 1.564 Å, which is nearly equal to 1.545 Å obtained by the

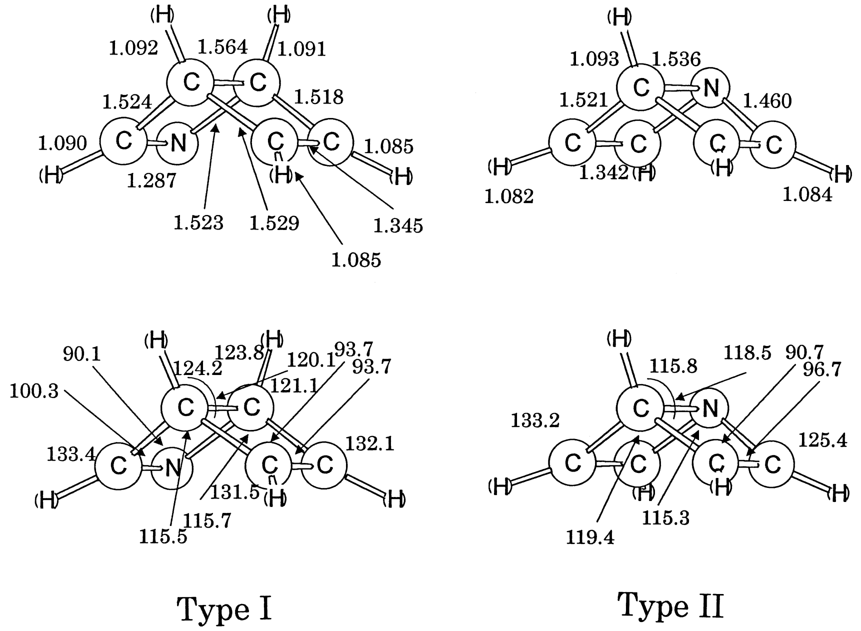

Fig. 4. Optimized geometrical structures of Dewar pyridine: bond lengths and angles are in angstroms and in degrees, respectively.

RHF calculation [17], but is slightly different from 1.590 Å obtained by the MP2 calculation [18]. This discrepancy may be caused by a smaller size of the basis set used in the MP2 calculation.

Vibrational wavenumbers and infrared absorption intensities have also been calculated for types I and II. The calculated spectral patterns are compared with the observed infrared spectrum in Fig. 2. The observed spectrum is similar to the spectral pattern of Type I, although the strong bands around 850 and 750 cm^{-1} split into three peaks. These splits, which were also observed by Johnstone and Sodeau [8], are probably due to Fermi resonance with combination bands related to the skeletal torsional modes. No split was observed in the spectrum of the deuterated species, as will be described later. On the other hand, the spectral pattern of Type II indicates that the most intense bands are expected to appear ca. 800 and 1050 cm^{-1}. This prediction is not consistent with the observed spectrum.

To our knowledge, there was no data on calculated and observed vibrational spectra for deuterated Dewar pyridine. The spectral patterns of C_5D_5N for types I and II have also been calculated and compared with the observed spectrum in Fig. 3. As in the normal species, the spectral pattern of Type I is closer to the observed spectrum than that of Type II. The calculated values of vibrational wavenumbers for Type I are compared with the observed values in Table 1 with relative intensities. The observed values are smaller than the corresponding calculated values by a few percent. This finding supports the empirical rule that a scaling factor of 0.96 is generally used in the DFT calculation. Judging from the foregoing relative energy and the spectral patterns, we conclude that Type I of Dewar pyridine is produced from pyridine in an argon matrix by UV irradiation.

3.3. Photodissociation to cyclobutadiene and HCN

Johnstone and Sodeau [8] reported that 253.7 nm photolysis of pyridine in an argon matrix generated a single product, namely Dewar pyridine. However, we observed a new band at 1243 cm^{-1} in our spectrum when UV irradiation on the matrix sample was prolonged. Fig. 5(a) shows the spectral changes observed at various UV irradiation times. The wavenumber of this band is nearly equal to 1245 cm^{-1} for the in-plane bending mode of cyclobutadiene reported by Arnold and Michl [19]. The corresponding band for completely deuterated species was observed at 1043 cm^{-1}, as shown in Fig. 5(b). Since Arnold and Michl [19] reported no experimental data on C_4D_4, we have performed a DFT calculation on cyclobutadiene at the same level as that used in the calculation for Dewar pyridine. The calculated wavenumbers for the in-plane bending mode, 1265 and 1054 cm^{-1} for C_4H_4 and C_4D_4 species, respectively, agree with the corresponding observed wavenumbers, 1243 and 1043 cm^{-1}. Therefore, we conclude that cyclobutadiene is produced from pyridine by further UV irradiation. The infrared bands of HCN, which is a counterpart of cyclobutadiene, were observed at 3230, 2093, and 756 cm^{-1} for the C–H stretching, C≡N stretching and HCN bending

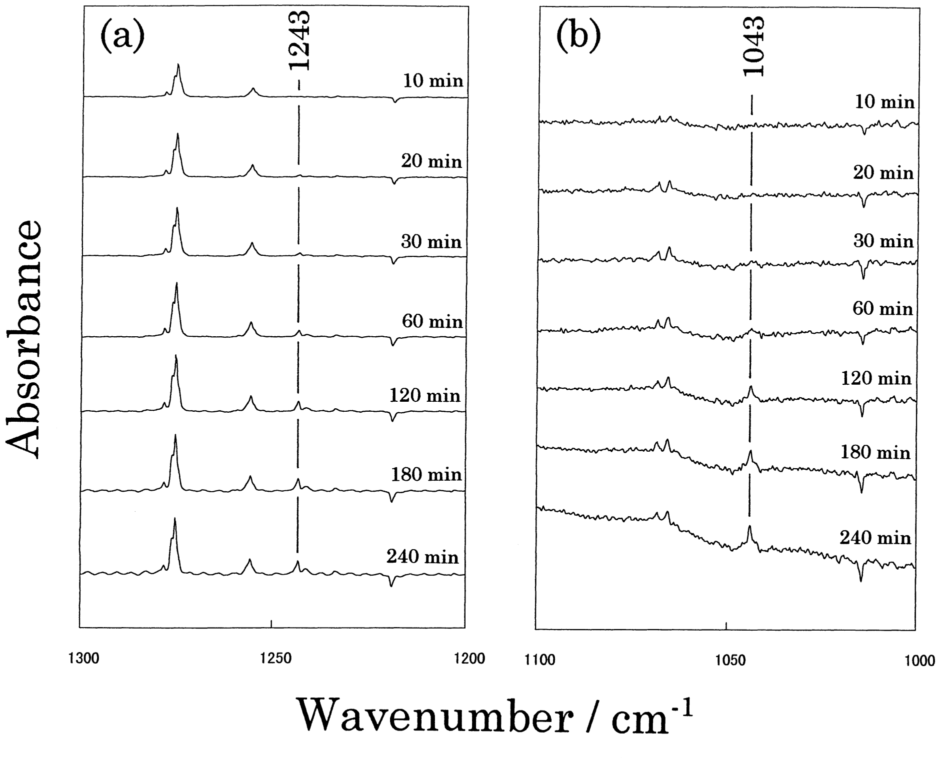

Fig. 5. Spectral changes upon long-time UV irradiation: (a) photolysis of C_5H_5N, the 1243 cm^{-1} band is due to cyclobutadiene; and (b) photolysis of C_5D_5N, the 1043 cm^{-1} band is due to cyclobutadiene-d_4.

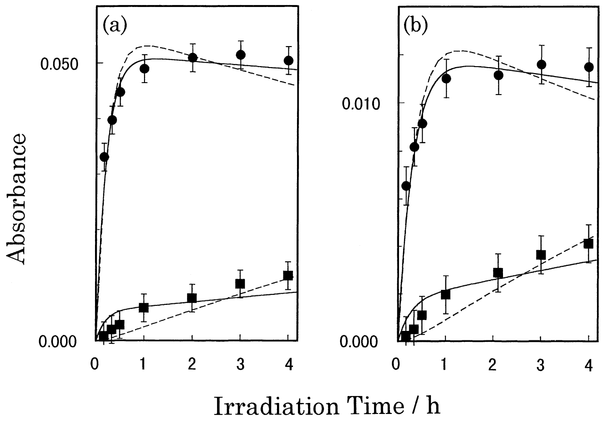

Fig. 6. Absorbance growth behavior of the infrared bands: (a) Photolysis of C_5H_5N. Symbols ● and ■ denote the 1275 cm^{-1} bands for Dewar pyridine and the 1243 cm^{-1} band for cyclobutadiene, respectively; (b) Photolysis of C_5D_5N. Symbols ● and ■ denote the 1115 cm^{-1} band for Dewar pyridine-d_5 and the 1043 cm^{-1} band for cyclobutadiene-d_4, respectively. Broken and solid lines represent the calculated values estimated by a least-squares fitting using Schemes 1 and 2, respectively.

modes, respectively. They seem to deviate somewhat from the corresponding values of HCN monomer in an argon matrix [9], 3306, 2098, and 721 cm^{-1}, probably because of intermolecular interaction between HCN and cyclobutadiene. The intensity changes of the bands for HCN were found to be nearly equal to those for cyclobutadiene. This finding means that HCN and cyclobutadiene are simultaneously produced by the UV photolysis.

3.4. Reaction mechanism

Fig. 6(a) shows intensity changes of the infrared bands at 1275 cm^{-1} for Dewar pyridine and 1243 cm^{-1} for cyclobutadiene upon UV irradiation. The intensity of the 1243 cm^{-1} band increases steeply in the beginning and, thereafter, decreases very slowly as the irradiation time increases. On the other hand, the intensity of the 1243 cm^{-1} band increases more slowly than that of Dewar pyridine. Recently, Prather and Lee [20] studied the mechanism of photodissociation of pyridine in the gas phase excited at 193 nm by photofragmentation translation spectroscopy. They observed HCN and C_4H_4 fragments and proposed a primary pathway to produce cyclobutadiene and HCN via Dewar pyridine as

Scheme 1 was also proposed by Chapman et al. [7], although they could not observe any spectra of Dewar pyridine. In our preliminary analysis on the kinetics, we assumed Scheme 1 to determine the rate constants k_1 and k_2 from the intensity changes of the infrared bands by a least-squares fitting. The absorbances of the bands for Dewar pyridine, A^{DP}, and cyclobutadiene, A^{CB}, are expressed as

$$A^{DP} = RA^{\infty}[k_1/(k_2 - k_1)][\exp(-k_1 t) - \exp(-k_2 t)] \quad (1)$$

$$A^{CB} = A^{\infty}\{1 + 1/(k_2 - k_1)[k_1 \exp(-k_2 t) - k_2 \exp(-k_1 t)]\}, \quad (2)$$

where A^{∞} and R represent the absorbance of cyclobutadiene at infinite irradiation time and the ratio of the absorption coefficients of Dewar pyridine and cyclobutadiene, respectively [21]. We estimated R to be 0.86 by the DFT calculation and treated k_1, k_2, and A^{∞} as parameters in the fitting. However, the observed values could not be reproduced within experimental errors; the estimated decrease in the band for Dewar pyridine was quicker and the increase in the band for cyclobutadiene was slower. We tried to fit the experimental data by varying the initial values, but it was impossible to fit them by Scheme 1 (broken line).

Then, we adopted Scheme 2, where cyclobutadiene and HCN are produced directly from pyridine in addition to the photodissociation of Dewar pyridine.

This scheme resembles the one used in our previous studies of visible-light induced photoreactions of NO_2/alkenes [22–27], NO_2/alkynes [28] and NO_2/alkadienes [29]. The absorbances of the bands for Dewar pyridine, A^{DP}, and cyclobutadiene, A^{CB}, were expressed as [22]

$$A^{DP} = RA^{\infty}[k_1/(k_2 - k_1 - k_3)] \times [\exp(-k_1 t - k_3 t) - \exp(-k_2 t)] \quad (3)$$

$$A^{CB} = A^{\infty}\{1 + 1/(k_2 - k_1 - k_3) \times [k_1 \exp(-k_2 t) - (k_2 - k_3)\exp(-k_1 t - k_3 t)]\}. \quad (4)$$

The rate constants, k_1, k_2, k_3 and the absorbance, A^{∞}, were treated as parameters in the fitting, whereas R was fixed to 0.86 estimated by the DFT calculation. The obtained values are 4.7 ± 0.5, 0.014 ± 0.013 and 0.43 ± 0.16 h^{-1} for k_1, k_2 and k_3, respectively, whereas A^{∞} is 0.066 ± 0.002. The uncertainty represents standard deviation calculated in the fitting. The constant k_2 is found to be smaller than k_1 by more than two orders. One of the reasons is that the intensity of the UV radiation from a superhigh-pressure mercury lamp depends on the wavelength. Since the absorption maximum of Dewar pyridine may shift to a shorter wavelength because of its non-conjugated π-electron system, the absorption coefficient of Dewar pyridine is probably lower than that of pyridine in the present experimental region. When the intensity changes of the bands for HCN are used in the fitting

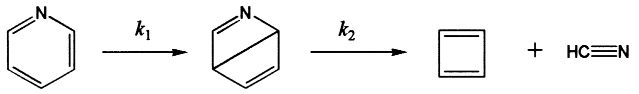

Scheme 1.

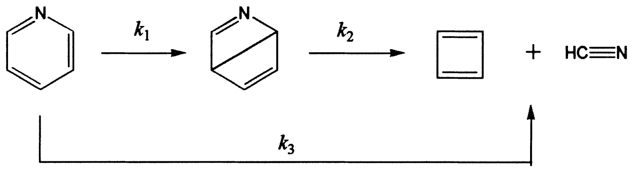

Scheme 2.

instead of those for cyclobutadiene, the obtained values were almost unchanged.

The k_3 constant is one order of magnitude smaller than k_1 but one order of magnitude larger than k_2. We conclude that most of cyclobutadiene and HCN are directly produced from pyridine, contrary to the mechanism proposed by Chapman et al. [7]. In this photodissociation process, Dewar pyridine seems to play a minor role. Therefore, the electronically excited state of pyridine to produce Dewar pyridine is possibly different from that for the direct photodissociation process into cyclobutadiene and HCN, for example, states of different spin multiplet. Johnstone and Sodeau [8] proposed a possible reaction pathway to produce Dewar pyridine through the lowest triplet state of pyridine. If their description is correct, cyclobutadiene and HCN may be produced through a singlet excited state. In order to understand the reaction mechanism in more detail, one must compare the corresponding quantum yields instead of the rate constants. Since the absorption coefficients of the photoproducts and intensities of the UV light from a superhigh-pressure mercury lamp were unknown in the present work, we have not been able to evaluate the quantum yields.

The intensity changes of the infrared bands of completely deuterated species are shown in Fig. 6(b). The rate constants were determined by the same procedure with an assumption of $R = 0.73$, as estimated by the DFT calculation. The obtained values are 3.3 ± 0.4, 0.025 ± 0.016, and $0.37 \pm 0.14\ \mathrm{h}^{-1}$ for k_1, k_2, and k_3, respectively, whereas A^{∞} is 0.019 ± 0.001. The A^{∞} of the normal species seems to be significantly larger than that of the deuterated species. This is consistent with the results of our DFT calculation, where the relative intensities of the $1243\ \mathrm{cm}^{-1}$ (normal species) and $1043\ \mathrm{cm}^{-1}$ (deuterated species) for cyclobutadiene are calculated to be 39 and 15, respectively. The k_1 and k_3 constants for the deuterated species seem to be smaller than those for the normal species. This fact implies the possibility that the absorption maximum of pyridine shifts to a shorter wavelength by deuteration.

4. Summary

Infrared spectra of normal and completely deuterated species for Dewar pyridine in low-temperature argon matrices were measured to determine the structures. Vibrational assignments were performed with an aid of the DFT calculation, where B3LYP/6-31++G** basis set was used to optimize geometrical structures. It was found that the calculated vibrational wavenumbers and infrared intensities for the C–C bridging tautomer could reproduce the observed spectra. Dewar pyridine was photolyzed by further UV irradiation to produce cyclobutadiene and HCN. Another reaction pathway to produce cyclobutadiene and HCN by direct photodissociation of pyridine was assumed. From the intensity changes of the infrared bands for Dewar pyridine and cyclobutadiene, the relative rate constants were determined by a least-squares fitting.

Acknowledgements

The authors wish to thank Professor Kozo Kuchitsu (Josai University) for his helpful discussion.

References

[1] J. Dewar, Proc. R. Soc. Edinburgh 82 (1866-1867).

[2] H.R. Ward, J.S. Winshnok, J. Am. Chem. Soc. 90 (1968) 5353.

[3] H.F. Shurrell, D.W. Griffith, J.E. Kent, J. Raman Spectrosc. 2 (1974) 147.

[4] D.W. Griffith, J.E. Kent, M.F. O'Dwyer, Aus. J. Chem. 28 (1975) 1379.

[5] E.A. McNeill, F.R. Scholer, J. Mol. Struct. 31 (1976) 65.

[6] D.W. Griffith, J.E. Kent, Chem. Phys. Lett. 25 (1974) 290.

[7] O.L. Chapman, C.L. McIntosh, J. Pacansky, J. Am. Chem. Soc. 95 (1973) 614.

[8] D.E. Johnstone, J.R. Sodeau, J. Phys. Chem. 95 (1991) 165.

[9] S. Kudoh, M. Takayanagi, M. Nakata, J. Mol. Struct. 413 (1997) 365.

[10] M. Nakata, Y. Somura, M. Takayanagi, K. Shibuya, T. Uchimaru, K. Tanabe, J. Phys. Chem. 100 (1996) 15815.

[11] S. Kudoh, M. Takayanagi, M. Nakata, T. Ishibashi, M. Tasumi, J. Mol. Struct. (in press).

[12] H. Yoshida, T. Harada, H. Matsuura, J. Mol. Struct. 413-414 (1997) 217.

[13] H. Yoshida, H. Matsuura, J. Phys. Chem. A 102 (1998) 2691.

[14] GAUSSIAN 94 was employed for the calculations. M.J. Frisch, G.W. Trucks, H.B. Schlegel, P.M.W. Gill, B.G. Johnson, M.A. Robb, J.R. Cheeseman, T.A. Keith, G.A. Petersson, J.A. Montgomery, K. Raghavachari, M.A. Al-Laham, V.G. Zakrzewski, J.V. Ortiz, J.B. Foresman, J. Cioslowski, B.B. Stefanov, A. Nanayakkara, M. Challacombe, C.Y. Peng, P.Y. Ayala, W. Chen, M.W. Wong, J.L. Andres, E.S. Replogle, R. Gomperts, R.L. Martin, D.J. Fox, J.S.Binkley, D.J. Defrees, J. Baker, J.P. Stewart, M. Head-Gordon, C. Gonzalez, J.A. Pople, Gaussian, Inc., Pittsburgh PA, 1995.

[15] A.D. Becke, J. Chem. Phys. 98 (1993) 5648.

[16] C. Lee, W. Yang, R.G. Parr, Phys. Rev. 37B (1988) 785.

[17] R. Liu, X. Zhou, P. Pulay, J. Phys. Chem. 96 (1992) 3669.

[18] J. Jones, G.B. Bacskay, J.C. Mackie, A. Doughty, J. Chem. Soc. Faraday Trans. 91 (1995) 1587.

[19] B.R. Arnold, J. Michl, J. Phys. Chem. 97 (1993) 13348.

[20] K.A. Prather, Y.T. Lee, Israel J. Chem. 34 (1994) 43.

[21] J.W. Moore, R.G. Pearson, Kinetics and Mechanism, John Wiley & Sons, New York, 1981.

[22] M. Nakata, H. Frei, J. Am. Chem. Soc. 111 (1989) 5240.

[23] M. Nakata, H. Frei, J. Phys. Chem. 93 (1989) 7670.

[24] M. Nakata, H. Frei, J. Chem. Soc. Japan (1989) 1412.

[25] M. Nakata, K. Shibuya, H. Frei, J. Phys. Chem. 94 (1990) 8168.

[26] M. Nakata, Spectrochim. Acta 50A (1994) 1455.

[27] M. Nakata, Y. Somura, M. Takayanagi, N. Tanaka, K. Shibuya, T. Uchimaru, K. Tanabe, J. Phys. Chem. 100 (1996) 15815.

[28] M. Nakata, H. Frei, J. Am. Chem. Soc. 114 (1992) 1363.

[29] N. Tanaka, Y. Kajii, K. Shibuya, M. Nakata, J. Phys. Chem. 97 (1993) 7048.